

Fluid structure in volcanic eruption column observed by Ka-band Doppler radar

*Takeshi Maesaka¹, Masayuki Maki², Tomofumi Kozono³

1.National Research Institute for Earth Science and Disaster Prevention, 2.Kagoshima University,
3.Tohoku University

Volcanic ash dispersion and falling with the explosive eruption affect aviation safety, so it is urgent necessary to develop its observation and prediction methods with high accuracy. For these problems, volcanic plume and ash dispersion modeling have been studied. The former physically solves the fluid-dynamical structure and the ash advection in the plume under the given condition of magma burst, however it is difficult to validate the results comparing with the observation data. The latter simulates the advection and dispersion of the ash, but the reliable initial conditions (e.g., three dimensional distribution of ash density) are needed for the accurate simulation. The ash observation by radar remote sensing are expected to be a solution for these problems.

So far some observational studies for the volcanic ash were demonstrated by using ordinary weather radar. But those could observe only relatively dense volcanic smoke, because radar reflectivity of the volcanic ash is smaller than that of the precipitation. In 2000, NIED developed Ka-band (35 GHz) Doppler radar, which can observe not only precipitations but also clouds. This radar is expected to detect the weak eruption. Moreover it is expected to retrieve a fluid structure in the smoke by detecting the Doppler effect of the radio wave. We deployed the radar at Kurokami branch observatory, Sakurajima Volcano Research Center, Kyoto University during March-June in 2014 for the observation of the Sakurajima eruption. In this presentation, our application of the meteorological radar analysis technique to the volcano eruption and the retrieved fluid dynamics will be reported.

Keywords: Volcanic eruption column, Meteorological Doppler radar, Ka-band

Microphysical Studies of Volcanic Ash Clouds by X-band Polarimetric Weather Radar Observation

*Masayuki Maki¹, Yura Kim², Dong-In Lee²

1.Observation and Prediction Research Department, Kagoshima University, 2.Pukyong National University

It has been recognized since the 1970's that weather radars can detect volcanic ash clouds. However, it is only since the 1990's that weather radars have been used in studies of quantitative ash cloud estimation. The present paper investigates the microphysical properties of volcanic ash clouds, the knowledge of which is necessary for quantitative ash cloud studies. Two volcanic eruptions at the Showa crater in Sakurajima, Kagoshima, Japan are analyzed. Both eruptions were observed by X-band operational polarimetric radar, which is installed by the Ministry of Land, Infrastructure, Transportation and Tourism approximately 11 km from the crater.

In the first eruption, which occurred on August 18, 2013, the ash column rose to a height of 5500 m above the crater. In the second eruption, which occurred on August 29, 2013, the ash echo and the precipitation echo coexisted. Analysis was performed on polarimetric radar parameters that were obtained by PPI scan at an elevation angle of 6 degrees. Radiating echo patterns, which extended from the north-northwest direction to the south-southeast direction through the crater, are found in the reflectivity factor (ZH) and the differential reflectivity (ZDR) immediately following the eruption. The direction of the radiating echo corresponds to that of a line connecting the radar and the crater. The radiating echo is probably due to the effect of the range side lobe of the transmitted pulses. A similar radiating pattern was also found in the correlation coefficient of the horizontal and vertical polarization (RHOHV) immediately after the eruption. The radiating echo patterns had almost disappeared by 6 minutes after the eruption. Interesting time changes of ZH and ZDR were found during the period from 6 minutes to 24 minutes after the eruption: While the ZH decreased with time, ZDR increased with time. The RHOHV values were 0.8-0.9 until 24 minute after the eruption. This value decreased to 0.7-0.8 at the central region of the echo and to less than 0.5 at the outer edge of the echo. On the other hand, the time change of the specific differential phase (KDP) of the ash smoke was quite different from those of the other polarimetric radar parameters: it was too small to be detected immediately after the eruption, while it was 0.5deg/km at 14 minutes after the eruption before increasing to about 1deg/km. The present paper explains these polarimetric radar parameter time changes by time changes of the microphysical properties of ash particles.

While the first eruption studied occurred in dry environmental conditions, the second occurred in wet conditions. Before the eruptions, precipitation echoes were generated to the west of Sakurajima and passed over Sakurajima immediately after the eruptions. The subject radar could detect the precipitation echoes and the eruption echoes independently. However, it was difficult to distinguish between the ash smoke and the precipitation because both ZH patterns were quite similar. We attempted to discriminate them using polarimetric radar parameters.

Keywords: radar, volcanic smoke, volcanic eruption, three dimensional

Information of volcanic ash material from satellite infrared sounder data

*Hiroshi Ishimoto¹

1. Meteorological Research Institute

Brightness temperature (BT) spectrums of the volcanic ash clouds in the IR window region measured by a satellite infrared sounder has been simulated in detail from the radiative transfer calculations by taking into account the appropriate atmospheric profiles, sea surface temperature/emissivity, atmospheric gas absorptions, and ash-scattering properties. From iterative least-square calculations using measured and simulated BTs, we made estimations of the ash refractive index (RI) as well as the ash cloud parameters (optical depth, particles effective radius, and ash cloud pressure heights). The absorption spectral feature of the RI in wavelength region around 10 micron depends on the Si-O bond characteristics of the erupted silicate material and therefore it is correlated with the mineral type and SiO₂ content. From the retrieval analysis, it is found that some estimated RIs were consistent with the reported rock types of the volcanoes, which had been previously classified by compositional analyses in the literature. Furthermore, weak absorptions likely due to Si-O and/or Al-O vibrations, which have been proposed in reports from previous laboratory FTIR experiments for some silicate glass samples were identified. The spectral RI estimated from the analyses of data from a satellite infrared sounder can be used to analyze other satellite measurements. In particular, information for the detailed RI in the infrared region contribute to ash cloud quantification and monitoring from measurements by next-generation geostationary satellites, such as the Japanese HIMAWARI-8. Moreover, it is possible to discuss the time evolution of components of the eruption products from changes in the RI estimated from IR sounder measurements.

Keywords: volcanic ash, satellite infrared sounder, refractive index

Influence to GNSS signals by volcanic ash plume

Sayo Ueshin¹, *Seiichi Shimada², Akira Takeuchi³

1.Faculty of Science, University of Toyama, 2.Graduate School of Frontier Sciences, University of Tokyo, 3.Graduate School of Sci. and Eng. For Education, University of Toyama.

Recently, GNSS data of the continuous observation system GEONET are utilized for monitoring and study of crustal deformation. Oota et al. 2013 presumed the GPS carrier phase balance residual and found conspicuous phase Post fit Phase Residual with the about 24 th July 2012 eruptive event in the Minami crater of Sakurajima Volcano by using PPP.

The purpose of this study is to presume LC PPR by using a same method as the above, and to deliberate the factor of LC PPR change. Eruptive event is a large typical volcanian that occurred at Shintake crater of Kuchinoerabujima on May 29, at 9:59 local time JST. Volcanic ash diffused from WNW to ESE.

This study analyzed the GEONET GPS data acquired on the observation station at Kuchinoerabujima by using GAMIT software ver.10.5.

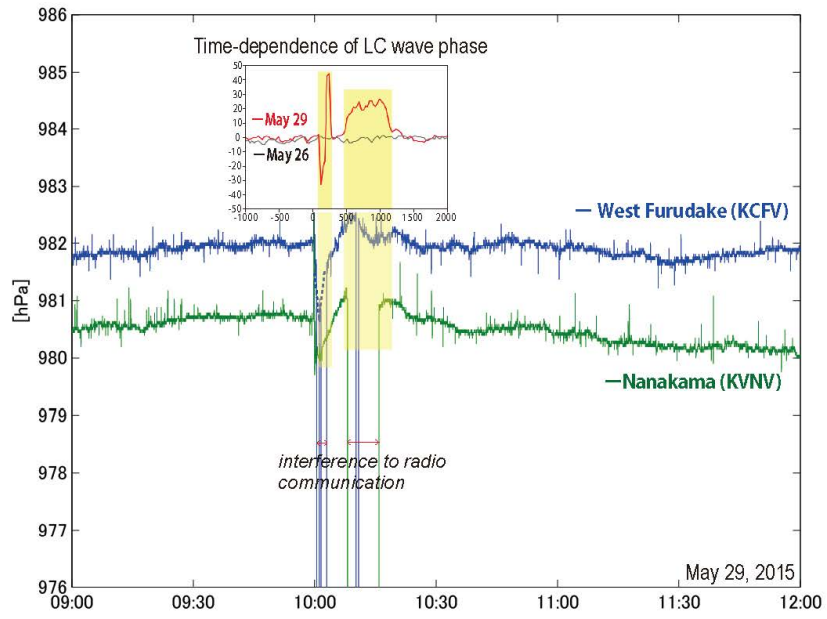
A result of the analysis, LC PPR of PRN18,22,26,29 changed conspicuously. LC PPR of PRN18,22,26 increase about 20cm. But It LC PPR of PRN29 decreases minus 32cm, and increases 42cm for during a short term, increases about 20cm for long term. These changes were almost synchronous with the abnormal changes of atmospheric pressure changes recorded at the northeastern foot of volcano. It is for the first time that the variation of such extreme LC phase residuals detected by this study along with volcanic eruption.

From the space images of the weather satellite HIMAWARI, it was confirmed that, just after the eruptive plume was started to form, the umbrella ash cloud was once spread around the volcanic body, and that the ash cloud flew from WNW to ESE direction. Checking both the behavior of this plume and the results of GAMIT analysis, it was found that radio waves from the PRN18,22,26 reached the observation station through

the spreading umbrella cloud, while those of PRN29 had reached through the eruption column.

Based on the video recording immediately after the start of the eruption and the timing of the communication failure of barometer system, rapid reduction and recovery of the air pressure or strong electrification including volcanic lightning, caused by over expansion of air accompanied with the sudden towering of plume pillars could account for the cause of the sharp minimum and maximum within a short time in the variation of LC PPR of PRN29 passed through the eruption column. Moreover, from the fact that the maximum of PRN29 was synchronous with the maximum of about 1 minute seen in PRN18,22,26 which passed through the spreading umbrella cloud, a possible factor for delay is considered due to water vapor increase or the temperature rise in the plume. For the broad increase in a long time of PRN29 was considered related to factors such as an increase of volcanic gas concentration, the subsequent rise in temperature or water vapor increase due to the diffusion of long plume umbrella.

The present study suggested a correlation between the events of the growth and towering of the volcanic plume and the LC PPR variation of GNSS radio waves. However, in order to elucidate the causes of changing the LC PPR it is necessary to perform a detailed study about the relationship between the LC PPR and dynamics of the eruption plume.



Transition process of parent cloud causing tornadoes accompanied by Typhoon, 'Neoguri'

*Soichiro Yuasa¹, Koji Sassa²

1.Graduate school of Integrated Arts and Sciences, Kochi University, 2.Natural Science Cluster, Kochi University

Two tornadoes simultaneously occurred near Kochi airport when the outer rainband of 'Neoguri' passed through the Kochi plain on 10 July 2014 (Yuasa and Sassa 2014). These tornadoes correspond to the vortices in their parent cloud, mc1 and mc2. The parent cloud was found to one of mini supercell when mc1 was observed at first. However, it did not have the feature of supercell when it landed (Yuasa and Sassa 2015). The present analytical study aims to clarify the transition process of the parent cloud with the data of Muroto Doppler radar.

We used the polar coordinates data of JMA Muroto radar obtained from NICT archives and analyzed with Draft software developed by MRI. We also used the initial GPV data of JMA meso scale model obtained from the RISH archives.

Fig.1 shows the PPI scan data of elevation angle 0.4 deg. Strong wind of over 38 m/s in Doppler velocity approached to the parent cloud from southwest and weak echo region was observed just south side of mc1 until just after mc2 appeared as shown in Fig. 1a,b. Moreover, the strong echo more than 40 dBZ formed hook like echo pattern around mc1. The diameter of mc1 was about 10 km which corresponded to that of mesocyclone. These features of the parent cloud in the horizontal plane show those of supercell though the arrangement of hook echo is opposite to that of normal supercell. The diameter of mc1 became rapidly smaller at 5:45 JST, and then strong echo in the south portion of the parent cloud left from the parent cloud and hook echo disappeared as shown in Fig. 1c. The strong echo in the south portion disappeared when the parent cloud landed and the cyclonic horizontal shear in which the southerly wind at the east side was stronger than that at the west side. The MSM data also showed the cyclonic horizontal shear in the outer rainband in which the parent cloud located (Yuasa and Sassa 2015).

Figure 2 shows the vertical cross section of the parent cloud around mc1. Just after the genesis of vortices, vault structure was clearly observed around mc1 as shown in Fig.2a,b. But, the strong wind of more than 30 m/s approaching to the vault from southwest became weakened at 5:41JST. Though the area of strong horizontal wind was still observed at 5:45JST after mc1 became smaller, vault structure already disappeared and the echo top was apart from mc1 as shown in Fig. 2c. The parent cloud did not have the feature of supercell at all when it landed but it had the cyclonic horizontal shear as shown in Fig. 2d.

Conclusively, the parent cloud was founded to have the feature of supercell at first and then lost it because the strong inflow from south. The cyclonic horizontal shear, however, still existed in the outer rainband and it kept the vortices. Finally, the tornadoes were kinds of non-supercell ones but their generation process was different from that of the ordinal non-supercell tornadoes (Wakimoto and Wilson 1989).

Keywords: radar observation, tornado, supercell

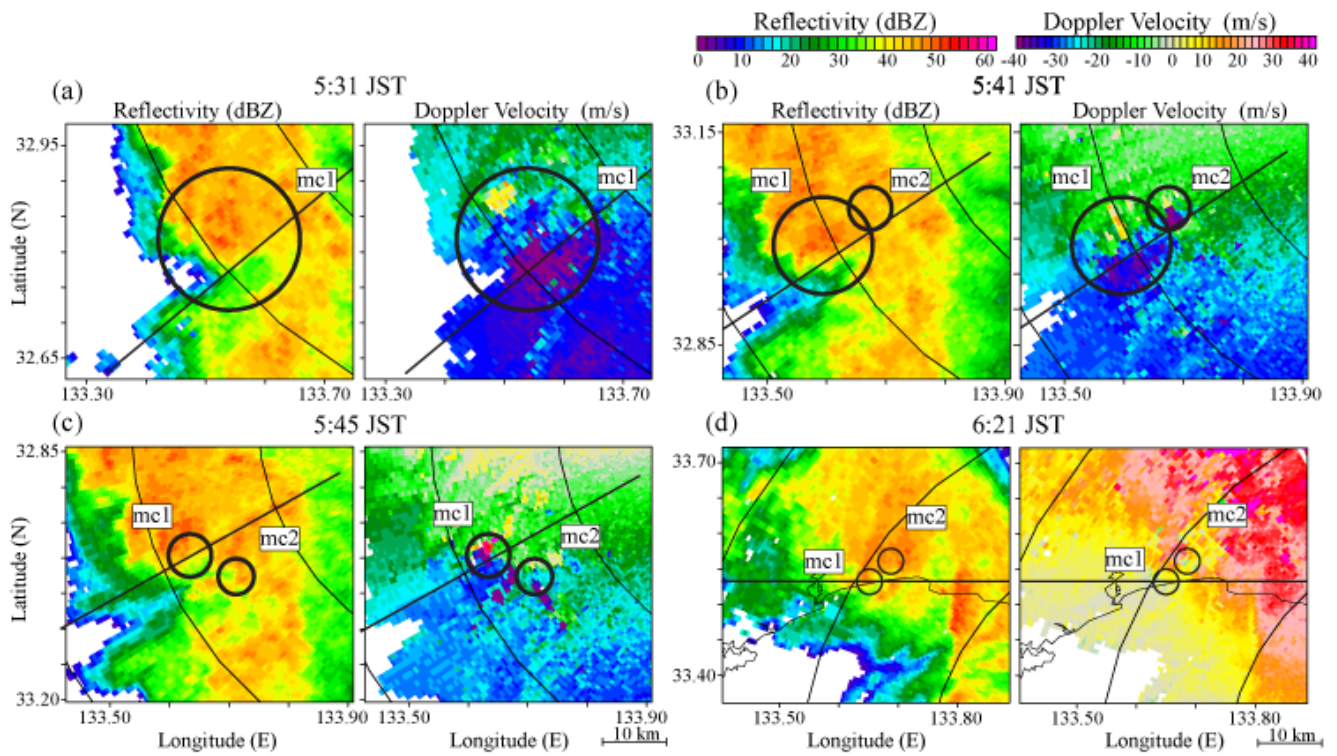


図1 渦発生後の室戸レーダー画像 (仰角 0.4deg)。 (左 ; レーダー反射強度 , 右 ; ドップラー速度) 図中丸はドップラー速度の極大極小から判断した渦付近を囲んだもの。 実線は図2の鉛直断面の領域。

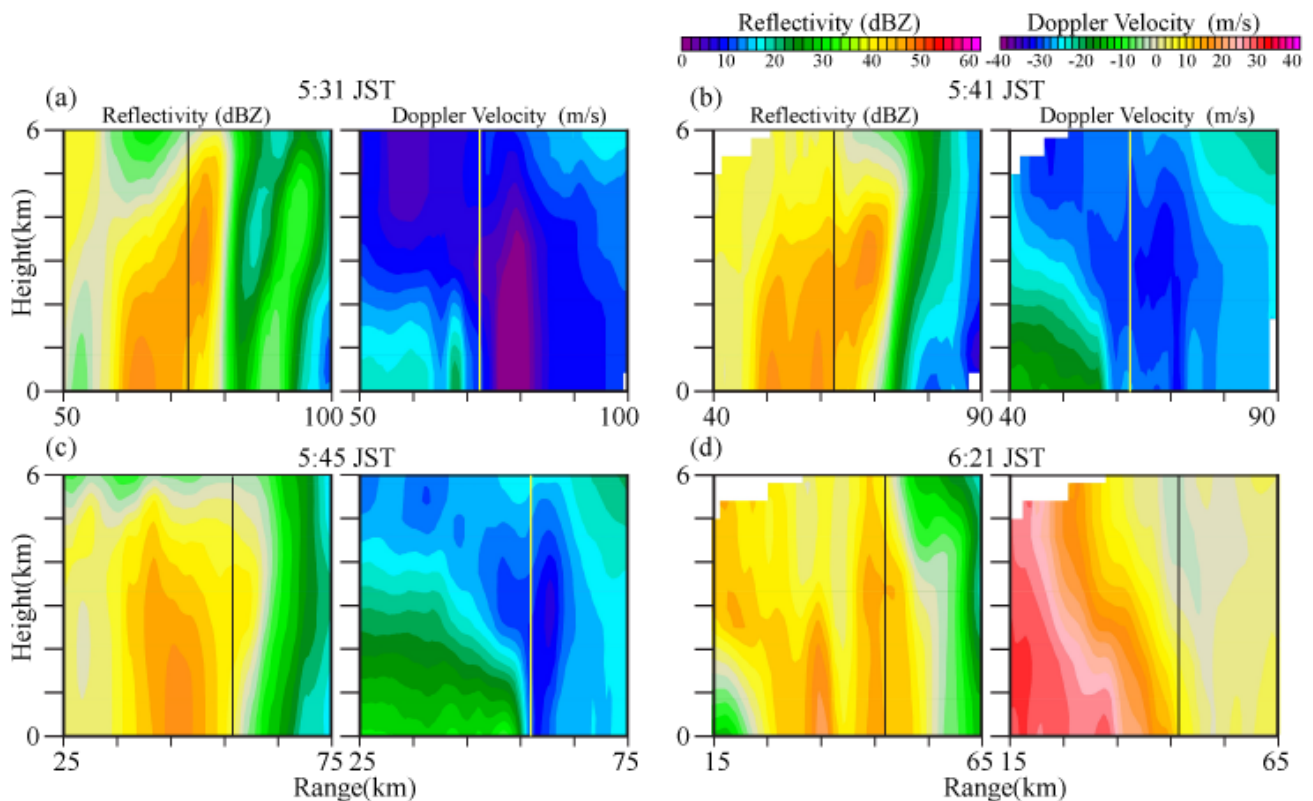


図2 mc1 渦中付近の室戸レーダーの断面図。図1の実線部 (30km) を高度 6km まで切出し、北から見た断面を示す。 実線は mc1 の渦中心。(左 ; レーダー反射強度 , 右 ; ドップラー速度)

Observation of Volcanic Ash Clouds by Himawari-8

*Yuta Hayashi^{1,2}, Daisaku Uesawa¹, Kotaro Bessho¹

1.Meteorological Satellite Center, Japan Meteorological Agency, 2.Meteorological Research Institute

Volcanic ash released by volcanic eruptions not only fall and accumulate on the ground over a wide area, but also float and disperse in the air for a long period. Since an encounter between aircrafts and volcanic ash clouds could result in a serious accident such as damage on the aircraft body and engine failure, information of distribution and altitude of volcanic ash clouds is essential for the safe operation of aircrafts. Geostationary meteorological satellites are one of the most important tools to monitor volcanic ash clouds, in the point that they can observe the wide range on the earth homogeneously and continuously.

Japan Meteorological Agency (JMA) began operation of the new-generation geostationary meteorological satellite, Himawari-8, on 7 July 2015. This year, JMA is also planning to launch Himawari-9, which is a backup system of Himawari-8. The imager on board is called Advanced Himawari Imager (AHI), whose observation performance is highly improved compared to that of the predecessor MTSAT-series satellites. For example, the number of observation bands is increased from 5 to 16, the spatial resolution is almost doubled, and the full-disk observation frequency is improved from hourly to every 10 minutes. Furthermore, for the small region including Japan, high-frequency observation as much as every 2.5 minutes is carried out. These high-resolution and high-frequency observations enable us to observe relatively small-scale and quickly changing phenomena, such as volcanic plumes and rapidly developing cumuli.

Volcanic ash clouds can be detected from satellite observation data using wave-length dependence of light absorbance of volcanic ash. With numerical weather prediction data and sea surface temperature data, we estimate volcanic ash cloud height, optical depth and several other quantities. Utilizing 16 bands observation data of Himawari-8, improvements in accuracy of volcanic ash clouds detection and estimation of those altitudes can be expected.

In this talk, I will show some cases of volcanic plume observed by Himawari-8. A basic concept of volcanic ash detection from satellite observations and how to generate volcanic ash RGB composite imageries will be explained. Additionally, I will briefly introduce satellite volcanic ash products which include physical quantities of volcanic ash clouds such as altitude and optical depth.

Keywords: volcanic ash clouds, remote sensing, geostationary meteorological satellite, Himawari-8

Current state and problems of field examination concerning tephra dispersal after pyroclastic eruptions

*Yasuo Miyabuchi¹

1. Faculty of Education, Kumamoto University

Dispersal pattern and volume or mass of tephra are fundamental factors determining type and magnitude of pyroclastic eruptions. However, the investigation method is outdated, and various problems exist to obtain highly precise data. This paper presents examples of field examination immediately after pyroclastic eruptions including Kirishima and Aso Volcanoes in Kyushu, SW Japan, and discusses the problems that appeared through the fieldwork.

The 2011 Shinmoedake eruption at Kirishima Volcano (southern Kyushu) was one of the largest eruption in Japan during the latest decade. Multiple subplinian eruptions occurred on January 26-27 and the tephra was dispersed throughout an area extending more than 20 km southeast from the source crater. Fieldwork was undertaken immediately after the eruption and a few months after the eruption. The eruption products were well preserved even a few months after the eruption, and it was possible to understand the tephra dispersal and correlate several fall units at different sites. Especially, it was clarified that the dispersal axis of the maximum size of pumice was slightly more northerly than that of thickness. This fact is consistent with the result of eruption plume simulation conducted by Suzuki et al. (2013). Our estimated volumes of the subplinian pumice-fall deposits on January 26-27 are one order of magnitude smaller than those of other studies probably because we use thickness data obtained at sites more than 2.5 km of the Shinmoedake crater. This suggests that proximal tephra data would be needed to give accurate estimates of the volume and mass of eruptive deposits.

Following the 1989-1995 eruptive sequence, multiple small ash emissions occurred at Nakadake crater, Aso Volcano (central Kyushu) in 2003-2008. A series of magmatic eruptions including ash, strombolian and phreatomagmatic eruptions occurred from November 2014 to December 2015. These eruptions provided valuable opportunities to examine eruption deposits in different volumes. It was useful to observe and sample ash deposited on artificial constructions or snow cover in the case of July 10, 2003 and January 14, 2004 small eruptions although it was difficult to recognize the ash on the natural surfaces.

In the initial stage of the 2014-2015 magmatic eruption at Nakadake, the ash-fall deposits could be easily observed and sampled on artificial surfaces at more than 40 sites, and the eruptive mass could be calculated using the isopleth map. Since subsequent ash-fall deposits could not be separated from the initial ash, ash samplers were installed at about 20 sites around the Nakadake crater. Although the ash observation system could be maintained, a big problem that fieldwork for ash sampling is restricted by road network has appeared. In the case of Nakadake, the eastern side of the crater is usually located downwind, and the downwind area has no road. Therefore, it is difficult to obtain the proximal data by fieldwork using cars. Moreover, it was experienced that ash sampling in the proximal area (<1 km of the crater) could not be often performed due to the risk of further eruptive activity. It is clarified that eruptive masses calculated by using both proximal and distal data are 1.4 times larger than those estimated by using only distal data. These evidences indicate that proximal tephra data would be needed to give accurate estimates of the volumes and masses of eruptive deposits as well as the 2011 Kirishima eruption.

As mentioned above, there is only one method to estimate distribution and mass of tephra deposits by fieldwork although the fieldwork immediately after pyroclastic eruptions has several serious problems. Therefore, it is expected to develop tephra plume simulation technique as well as

geological examination to give accurate estimates of eruptive volume and mass.

Keywords: pyroclastic eruption, tephra dispersal, eruptive volume

Reconstruction and estimation of physical parameters of a phreatic eruption on 27 September 2014 at Ontake volcano, Central Japan, based on pyroclastic density current and fallout deposits

*Fukashi Maeno¹, Setsuya Nakada¹, Teruki Oikawa², Mitsuhiro Yoshimoto³, Jiro Komori⁴, Yoshihiro Ishizuka², Yoshihiro Takeshita⁵, Taketo Shimano⁶, Takayuki Kaneko¹, Masashi NAGAI⁷

1.Earthquake Research Institute, University of Tokyo, 2.Geological Survey of Japan, AIST, 3.Mount Fuji Research Institute, Yamanashi Prefectural Government, 4.Faculty of Modern Life, Teikyo Heisei University, 5.Institute of Education, Shinshu University, 6.Graduate School of Environmental and Disaster Research, Tokoha University, 7.National Research Institute for Earth Science and Disaster Prevention

The phreatic eruption at Ontake volcano on 27 September 2014, which caused the worst volcanic disaster (58 deaths and 5 missing persons) in Japan in the past half-century, was reconstructed based on observation of proximal pyroclastic density current (PDC) and fallout deposits. Witnesses' observations were also used to clarify the eruption process. The deposits are divided into three major depositional units (Units A, B, and C) which are characterized by massive, extremely poor-sorted, and multimodal grain-size distribution with 30-50 wt.% of silt to clay component. The depositional condition was initially dry but eventually changed to wet. Unit A originated from gravity-driven turbulent PDCs in the relatively dry, vent-opening phase. Unit B was then produced mainly by fallout from a vigorous moist plume during vent development. Unit C was derived from wet ash fall in the declining stage. Ballistic ejecta continuously occurred during vent opening and development. As evidenced in the finest population of the grain-size distribution, aggregate particles were formed throughout the eruption, and the effect of water in the plume on the aggregation increased with time and distance. The lithofacies and grain-size characteristics of the poorly-sorted deposits observed in the proximal area are similar to those of mudflows or fallout tephra from past phreatic events. It is important to understand the similarity of the deposits when we interpret this type of poorly-sorted deposit solely based on geological records. Using geological records, witness observations, and a theoretical approach, the physical parameters of the Ontake eruption can be constrained. Based on the deposit thickness, duration, and grain-size data, the particle concentration and flow velocity for three PDC lobes in the initial phase were estimated to be 2×10^{-4} to 2×10^{-3} and 24-56 m/s, respectively, applying a scaling analysis using a depth-averaged model of turbulent gravity currents flowing down slopes. The tephra-thinning trend shows a steeper slope in the proximal area than on the trends of similar-sized magmatic eruptions, indicating a large tephra volume deposited over a short distance owing to the wet dispersal conditions. The Ontake eruption provided an opportunity to examine the deposits from a phreatic eruption with a complex eruption sequence that reflects the effect of external water on the eruption dynamics. Further studies may enable to quantitatively evaluate the major factors that caused the many casualties and severe damage to buildings near the eruption source.

Keywords: phreatic eruption, Ontake, pyroclastic density current, pyroclastic fallout, grain-size distribution

Transport and resuspension of ash particles from the 2014 phreatic eruption at Ontake Volcano, inferred by pollen sensor data

*Takahiro Miwa¹, Masashi NAGAI¹, Ryohei Kawaguchi¹

1.National research institute for earth science and disaster prevention

Behavior of ash particle from explosive eruptions is considered to influence many environmental and economic factors (e.g., Rose and Durant, 2011). Field survey on eruptive deposit have been performed to evaluate the behavior of ash particles and obtain ground truth for numerical simulation and satellite observation during explosive eruption (e.g., Gudmundsson et al. 2012). However, it is generally difficult to reconstruct timing and strength of ash transport from the field survey for small phreatic eruption, because ash deposit by such small eruption is easy to suffer reworking by wind and rain water. So, method which can detect ash particles *in situ* is favorable to infer the behavior of ash particles during the small phreatic eruption.

We examined time series data of pollen sensor to infer the transport and resuspension of ash particles from the 2014 phreatic eruption at Ontake volcano. The pollen sensor has been developed for *in situ* detection of pollen particle which causes allergy. The pollen sensor (PS2 by Shinyei technology Co. Ltd) is laser optical analyzer for particle matters, and consists of one light emitter and two light receptors. The particles are introduced into the chamber, and shot by linear polarized light emitted by the light emitter. The number of particles introduced into the chamber by intake of air are counted from the number of outputs recorded by a receptor every second. The combination of output voltage from the two receptors brings in a polarization factor (PF) reflecting shape of the particle matter. The polarization factor of pollen and water drop with spherical shape are higher (around 0.3 and 0.8) than that of soil particle from Kanto plain (around 0) (see HP of Shinyei technology Co. Ltd).

We analyzed pollen sensor data recorded by NTT Docomo Ltd from September 21th to October 19th, 2014 with a sampling frequency of 1 Hz at Kaida-kogen site which locates 11 km away from the summit of Ontake volcano. To remove the particle counts due to pollen and water drop, we recalculated hourly counts of particles having < 0.3 of polarization factor. Strong noise of the particle count prevents us to insight into behavior of ash particles in other 150 pollen sensor sites around Ontake volcano.

The time series of pollen sensor data from Kaida-Kogen allows us to infer the transport and resuspension processes of ash particles from the phreatic eruption. We find a sudden increase of the hourly count of particle matter with low polarization factor changing from few tens to maximum value of 5355 particles at 12:00-13:00 September 27th. Because the onset of the 2014 phreatic eruption at Ontake is 11:52 Sep 27th, we consider that unusual supply of particle matter by the eruption causes the sudden increase. In detail, count value by ten minutes interval provides maximum value of the count 80 minutes after the phreatic eruption. So, transport velocity of ash particles can be estimated to 2.3m/s which is comparable with velocity of local wind around the Ontake volcano. After the sudden increase, the particle count gradually decreases with some fluctuations, and becomes few particles per hour within 1 week. The fluctuations are well correlated with temporal variation of wind velocity in Kaida-Kogen, showing wind blowing induces resuspension of ash particles. Because the wind direction at the fluctuation are randomly oriented, we consider that ash particles on the leaf, tree and load around pollen sensor were resuspended by the wind blowing. Finally, we conclude that pollen sensor data can be used to evaluate behavior of ash particles even in small phreatic eruption.

Keywords: Volcanic ash, Pollen sensor, Phreatic eruption

An examination of the impact of initial size distribution of volcanic ash particles on volcanic ash transport simulation in the case of Shinmoe-dake eruption 2011

*Akihiro Hashimoto¹, Yujiro Suzuki², Toshiki Shimbori¹, Kensuke Ishii¹

1.Meteorological Research Institute, Japan Meteorological Agency, 2.Earthquake Research Institute, The University of Tokyo

The volcanic ash cloud appeared during the eruption event at Mt. Shinmoe-dake from 26 to 27 January 2011 was simulated using Japan Meteorological Agency Non-Hydrostatic Model (JMA-NHM), which is coupled with a volcanic ash source model, to validate the model performance, based on satellite observation data. The source model was made up of a function of the height at which ash particles are released and the size of particle, based on Suzuki, (1983) and Shimbori et al., (2010).

Applying the model to the volcanic ash transport simulation, reproducibility of the observed ash cloud was insufficient, because the model assumes a vertical eruption column that is not affected by cross wind and a simple air velocity profile in the eruption column, while the actual eruption event occurred in the environment with vertically sheared cross wind and the air flow in eruption column is not so simple as assumed in the model. To overcome the shortcomings of the model, new source model was developed based on the three-dimensional direct numerical simulation of a major sub-Plinian eruption during the period at Mt. Shinmoe-dake (Suzuki and Koyaguchi, 2013). The new model releases more ash particles in the middle troposphere than the usual model. This brought improvement of the reproducibility of the ash cloud.

For more improvement of the simulation result, the authors are examining the sensitivity of the resulted ash cloud distribution to another factor prescribed in the model; the initial size distribution of ash particles. As a preliminary result, it is found that doubling the variance of log-normal size distribution of ash particles improves the resulted ash cloud distribution. A systematic examination and its results on the impact of the initial size distribution on the ash transport simulation will be presented at the meeting.

Acknowledgement

This study was supported by the Earthquake Research Institute cooperative research program.

References

- Shimbori, T., Y. Aikawa, K. Fukui, A. Hashimoto, N. Seino, and H. Yamasato, 2010: Quantitative tephra fall prediction with the JMA mesoscale tracer transport model for volcanic ash: A case study of the eruption at Asama volcano in 2009. *Pap. Met. Geophys.*, 61, 13-29.
- Suzuki, T., 1983: A theoretical model for dispersion of tephra. *Arc Volcanism: Physics and Tectonics. TERRAPUB*, 95-113.
- Suzuki, Y. and T. Koyaguchi, 2013: 3D numerical simulation of volcanic eruption clouds during the 2011 Shinmoe-dake eruptions. *Earth Planets Space*, 65, 581-589.

Keywords: volcanic ash transport and dispersion model, Shinmoe-dake volcano, particle size distribution

Estimation method of tephra deposition using photovoltaic power generation data for model validation of tephra fall simulation.

*Fumichika Uno^{1,2}, Toshiki Shimbori², Akihiro Hashimoto², Hideaki Ohtake^{1,2}, Tetsuyuki Ishii³

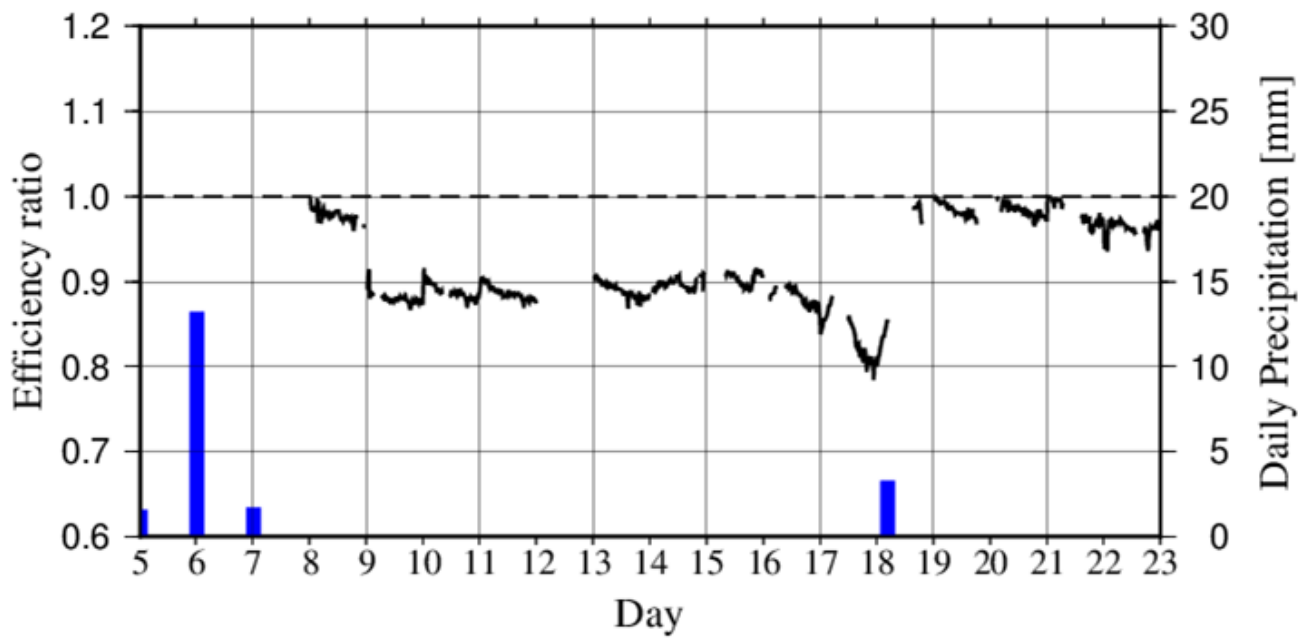
1.National Institute of Advanced Industrial Science and Technology, 2.Meteorological Research Institute, 3.Central Research Institute of Electric Power Industry

Operational and research-based tephra fall forecast and hindcast were performed for recent major eruption events in Japan using tephra transport and dispersion models. For a model validation, several data sets are already available such as the space-borne and ground-based remote sensing data as well as in-situ measurement data, however the temporal and spatial resolutions of those data are insufficient for precise quantitative evaluation of tephra fall. It is desired to develop new data representing tephra fall in higher resolution.

The authors propose an application of photovoltaic (PV) power data to estimation of tephra fall. Kaldellis and Kapsali (2011) indicated linear relationship between tephra deposition amount and PV power efficiency. In generally, numerous PV systems have been installed in the Japan and its PV output data has been also monitored at several minute intervals. This approach makes it possible to obtain the tephra fall data in high resolution without new instruments.

We investigated a relationship between tephra deposition and PV module efficiency at Kirishima exposure site in Kyusyu region (on the western part of the Japan islands) in July 2013. In case of a volcanic eruption event of Mt. Sakura-jima (on the southern part of Kyusyu region), it was confirmed that PV power output was on the decrease. PV power output restituted after rainfall event in 18 July, (see Figure). The number of events that PV power output was decreased more than 20 % compared with an initial condition is 72 days in 2013.

Keywords: Estimation of tephra fall, Photovoltaic power generation



Figure, Comparison of time series of PV module efficiency and daily-accumulated precipitation in July 2013. The solid black line indicate PV module efficiency (see left axis), and blue bar indicate daily precipitation (see right axis, mm), respectively.

The feasibility study for the estimating the grain-size distribution of volcanic ashes with the wind profiler LIDAR

*Shunsuke Hoshino^{1,2}, Toshiki Shimbori², Keiichi Fukui², Kensuke Ishii², Eiichi Sato², Shomei Shirato³, Kenji Fujiwara⁴, Yukio Komazaki^{1,2}

1.Aerological Observatory, 2.Meteorological Research Institute, 3.Japan Meteorological Agency, 4.Kagoshima Local Meteorological Office

There are some earlier studies of the observations of volcanic plume with the Mie LIDAR, such as Sakai et al. (2014), and most of them reported about the altitude of the volcanic-ash cloud, but there are not much studies about estimating the grain-size distribution of the volcanic ashes in troposphere with LIDAR. Doppler LIDARs are used to estimate the wind profile using the spectral analysis of the backscatter by aerosols. Aoki et al. (2015 a,b) demonstrate the estimation of rain drop size distribution using Gaussian Mixture Model (GMM) fitting of Doppler spectra. This suggests the possibility of the estimation of the grain-size distribution of aerosols.

As part of the joint research project by Meteorological Research Institute and Kagoshima Meteorological Office, the observation of wind around Sakurajima volcano using the Wind Profiler LIDAR (Doppler LIDAR, hereafter WPL) was done on March, 2015. The eruptions were observed by 32 times in the observation period, so WPL observed the atmospheric flow including volcanic-ash. In this study, the estimation method of volcanic ashes size distribution using spectral analysis is tested.

At first, the observed spectral power distributions are fitted to GMM, and derived Doppler speed (V_r) for each mode. The falling velocities of ashes (V_f) are derived from V_r and the environmental wind (V_e). The grain-sizes of ashes (D) are estimated using the relationship of D and V_f in Shimbori et al. (2014). In this study, the analysis data of the Japan Meteorological Agency (JMA) Local Forecast Model (LFM) are used as V_e . For the verification, the analyzed distribution is compared with one using the volcanic-ash prediction of the JMA Regional Atmospheric Transport Model (RATM) driven by LFM.

In the case study for the data between 14:50 -15:00 JST on 26th March, the peak of the distribution is about 0.1mm in the both results of WPL analysis and RATM prediction, so they are almost consistent. But the D in WPL analysis is widely distributed, up to 20mm. This 'unreliable' D is thought to be caused by the noise in spectra. In addition, some possible reasons to affect the analysis like the fluctuations of wind and the difference between the 'real' wind over WPL and the LFM analysis data must be considered. And the observed grain-size distribution data is needed for the further verification.

Although there are some points to be noted like the measures to the accumulation of falling volcanic-ashes on WPL antenna in the observation of the volcanos, there are advantages like the portability and the possibility to observe the lower wind profile. So it is worth to consider the applications WPL to the observation of the volcanic plumes.

Keywords: Volcanic ashes, Doppler LIDAR